Available online at www.sciencedirect.com
SCIENCE DIRECT
Tectonophysics 413 (2006) 39–52
TECTONOPHYSICS
www.elsevier.com/locate/tecto

An observational test of the stress accumulation model based on seismicity preceding the 1992 Landers, CA earthquake

Shoshana Z. Levin [a,*], Charles G. Sammis [b,1], David D. Bowman [c,2]

[a] Department of Earth Sciences, University of Western Ontario, London, Canada ON N6A 5B7
[b] Department of Earth Sciences, University of Southern California, Los Angeles, CA 90035-0740, USA
[c] Department of Geology, California State University, Fullerton, Fullerton, CA 92834-6850, USA

Received 28 October 2004; received in revised form 14 May 2005; accepted 4 October 2005
Available online 13 December 2005

Abstract

We test the Bowman and King [Bowman, D.D., King, G.C.P., 2001a. Accelerating seismicity and stress accumulation before large earthquakes. Geophys. Res. Lett., 28 (21), 4039–4042, Bowman, D.D., King, G.C.P., 2001b. Stress transfer and seismicity changes before large earthquakes. C. R. Acad. Sci. Paris, 333, 591–599] Stress Accumulation model by examining the evolution of seismicity rates prior to the 1992 Landers, California earthquake. The Stress Accumulation (SA) model was developed to explain observations of accelerating seismicity preceding large earthquakes. The model proposes that accelerating seismicity sequences result from the tectonic loading of large fault structures through aseismic slip in the elasto-plastic lower crust. This loading progressively increases the stress on smaller faults within a critical region around the main structure, thereby causing the observed acceleration of precursory activity. A secondary prediction of the SA model is that the precursory seismicity rates should increase first at the edges of the critical region, with the rates gradually rising over time at closer distances to the main fault. We test this prediction by examining year-long seismicity rates between 1960 and 2004, as a function of distance from the Landers rupture. To quantify the significance of trends in the seismicity rates, we auto-correlate the data, using a range of spatial and temporal lags. We find weak evidence for increased seismicity rates propagating towards the Landers rupture, but cannot conclusively distinguish these results from those obtained for a random earthquake catalog. However, we find a strong indication of periodicity in the rate fluctuations, as well as high correlation between activity 130–170 km from Landers and seismicity rates within 50 km of the Landers rupture temporally offset 1.5–2 years. The implications of this spatio–temporal correlation will be addressed in future studies.

Keywords: Accelerating moment release; Seismicity rates; Landers; Stress accumulation

1. Introduction

An increase in the number of intermediate events has been observed to precede nearly all California earthquakes with recorded magnitudes $M \geq 6.5$ (Ellsworth et al., 1981; Sykes and Jaumé, 1990; Knopoff et al., 1996; Bowman et al., 1998; Bowman and King, 2001a,b). Evidence of precursory accelerating seismicity from other regions includes observations of increased seis-

* Corresponding author. Fax: +1 519 661 3198.
E-mail addresses: slevin2@uwo.ca (S.Z. Levin), sammis@earth.usc.edu (C.G. Sammis), dbowman@fullerton.edu (D.D. Bowman).
[1] Fax: +1 213 740 8801.
[2] Fax: +1 714 278 7266.

0040-1951/$ - see front matter © 2005 Elsevier B.V. All rights reserved.
doi:10.1016/j.tecto.2005.10.032

micity rates before the 1707 Kwanto and 1923 Tokyo, Japan earthquakes (Lindh, 1990), and preceding large earthquakes in the Aleutian Islands (Bufe et al., 1994), and accelerating moment release prior to large New Zealand events (Robinson, 2000). The expectation of precursory accelerating seismicity can be derived from the principles of damage mechanics, which suggest that the cumulative seismic activity ($\sum\Omega$), measured as the number of events, moment or energy released, follows a power-law relationship with the time to failure:

$$\sum \Omega = A + B(t_f - t)^m, \quad (1)$$

where t_f is the predicted failure time of the large earthquake, and A, B and m are constants (Bufe and Varnes, 1993). Most studies represent Ω as the Benioff Strain, defined as the square-root of the energy released by each event.

This approach has been used to retrospectively forecast past large events, such as the 1989 Loma Prieta, CA earthquake (e.g., Bufe and Varnes, 1993), large southern California events since 1950 (e.g., Bowman et al., 1998; Bowman and King, 2001a,b), intermediate to large earthquakes in northern Baja California, Mexico (Sammis et al., 2004), and large New Zealand events (Robinson, 2000). Bowman et al. (1998) further demonstrate that the accelerating moment release (AMR) signal is maximized within a critical region that scales with the magnitude of the concluding large event. The usefulness of AMR in prospective forecasting has also been explored for activity in southern California (Bowman et al., 2003; Clark et al., 2003), and in the Aleutian Islands, with the successfully forecasting the 1996, M 7.9 Delarof Islands earthquake (Bufe et al., 1994).

Several models have been proposed to explain the precursory AMR phenomenon, including Intermittent Criticality (e.g., Sornette and Sammis, 1995; Huang et al., 1998; Bowman et al., 1998; Sammis and Smith, 1999; Anghel et al., 2000; Rundle et al., 2002; Bowman and Sammis, 2004), Damage Mechanics (e.g., Sammis et al., 1996; Lyakhovsky et al., 1997; Ben-Zion and Lyakhovsky, 2002), Epidemic-Type Aftershock Sequence (ETAS) (e.g., Kagan and Knopoff, 1987; Ogata, 1988, 1993; Helmstetter and Sornette, 2002, 2003; Helmstetter, 2003), and Stress Accumulation (Bowman and King, 2001a,b; King and Bowman, 2003). Each of these models suggests other, differing features that would be expected of the precursory seismicity and that might be incorporated in intermediate-term earthquake forecasts. In this paper, we examine the prediction of the Stress Accumulation model that within the critical precursory region of a large earthquake, an increase in seismicity rates should migrate over time towards the mainshock rupture.

The Stress Accumulation (SA) model of accelerating seismicity (Bowman and King, 2001a,b; King and Bowman, 2003) is an outgrowth of the Intermittent Criticality model (Bowman et al., 1998; Bowman and Sammis, 2004). It adds to the IC model a characterization of the spatial features of precursory seismicity, based on H. F. Reid's elastic rebound model (Reid, 1910) and Coulomb stress interactions. The Intermittent Criticality model states that during the interevent time of large events, the regional stress field becomes increasingly correlated. At any given moment, the largest earthquake the fault network can generate depends on the correlation length of the stress field. When the correlation length reaches the scale of the network, a large or "system-size" event becomes possible. The large earthquake, in turn, destroys the correlation, thereby resetting the system. In the SA model, AMR is related to the developing correlation of the stress field and to the specific pattern of stress accumulation leading up to the next large event. The SA model in its most basic form considers a sub-region broken by a single main fault that extends to lower crustal depths, and many smaller faults that are contained in the brittle upper crust. The central portion of the main fault remains locked between large earthquakes, while tectonic loading is released by a combination of seismic or aseismic slip on adjacent fault segments and creep on a planar extension of the fault at depth. Activity on the smaller surrounding structures occurs primarily in response to the accumulation and release of stress along the locked portion of the main fault.

The following sequence of 4 stages is predicted for the evolution of the stress field over the course of a mainshock cycle: 1) A major event on the main fault structure releases stress in some portions of the surrounding crust and transfers stress to others. Where the stress has decreased on the secondary faults (in the stress shadow), the seismicity rate drops significantly. Aftershocks and triggered events tend to cluster in the zones where the stress increased. 2) Aftershocks of the main event gradually relax the high stress zones, returning the stress to typical interseismic levels. Simultaneously on the main fault, tectonic loading generates motion on the lower crustal extension and on the segments adjacent to the locked portion, thereby eroding the stress shadow from the previous mainshock. Since the amplitude of the stress shadow is generally largest near the mainshock and decreases outward, the stress shadow erodes gradually from the outer edges of the affected region inward toward the fault. 3) Continued

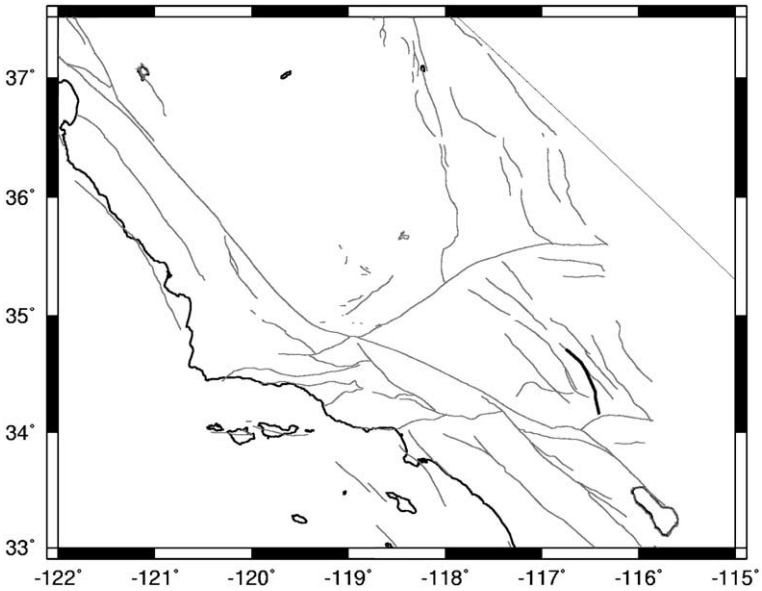

Fig. 1. Fault map of southern California. The 5 segments forming the fault trace of the Landers rupture model are highlighted in bold.

tectonic loading begins to increase the stress above the mean background level in zones roughly comparable to the previous stress shadows. The increasing area in which seismicity is being generated, combined with the increase in the maximum magnitude of events permitted by the growing correlation length of the stress field, yields the observed acceleration of precursory moment release. 4) When the stress shadow has been completely erased, the next major event occurs and the cycle restarts.

The SA model suggests features of precursory seismicity, in addition to AMR, which are testable with

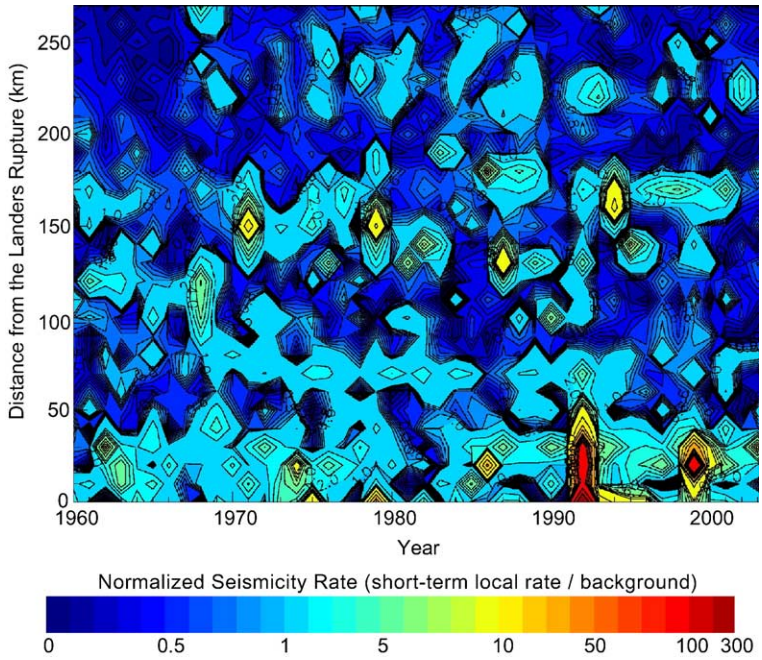

Fig. 2. Yearly seismicity rates as a function of distance from the Landers rupture, normalized by the long-term, regional background rate. The background rate is calculated using the entire 1960–2004 catalog of $M \geq 3$ events. The seismicity rates are contoured using a pseudo-logarithmic scale, in order to accommodate the wide range of values.

network catalog data. As explained above, the SA model predicts that the stress shadow from the previous great earthquake on a given fault structure erodes gradually over time. Since the amplitude of the drop in Coulomb failure stress caused by the prior event decreases with distance from the rupture, the temporal erosion of the stress shadow has an associated spatial component; the shadow erodes inward towards the main fault. Since the rise in stress levels is expected to promote seismic activity (Dieterich, 1994), the spatial evolution of the stress field should produce a corresponding pattern in the evolution of local seismicity rates. Specifically, an increase in seismicity rates should be observed at progressively closer distances to the mainshock fault as time approaches the next major event.

We test this prediction by examining seismicity rates before and after the June 28, 1992, Landers, CA earthquake. At magnitude 7.3, Landers is the largest earthquake to have occurred in California since the 1950s, and it is preceded by three decades of good network recording of small and intermediate events. Furthermore, the studies that developed the SA model document AMR prior to the Landers earthquake (Bowman and King, 2001a,b). Consequently, other phenomena predicted by the SA model should be observed for this event.

2. Methodology

We use the ANSS Composite Earthquake Catalog, available through the Northern California Earthquake Data Center (http://quake.geo.berkeley.edu/cnss/.). Our dataset includes events of magnitude $M \geq 3$, occurring from January, 1960 through December, 2004, in the region defined by the latitude range 31.5° to 37.5° and the longitude range −113° to −122°. The Gutenberg–Richter frequency–magnitude statistics indicate that the catalog is complete above magnitude 3.0 for this time period. The total dataset contains 135,863 earthquakes.

For the mainshock in our analyses, we use the Landers earthquake. The event occurred on June 28, 1992,

Table 1
Coefficients for the lag-shifted auto-correlation of the normalized seismicity rates for the earthquake catalog, 1960–2004 (Fig. 2)

Lag	0	1	2	3	4	5	6	7	8	9	10	11	12	13	14	15	16	17	18	19	20	21	22	23
−14	xx	xx	0.21	0.14	xx	xx	xx	xx	xx	xx	xx	xx	xx	xx	xx	xx	0.16	xx	xx	xx	0.22	xx	xx	xx
−13	0.07	xx	0.12	xx	xx	xx	xx	xx	xx	xx	xx	xx	xx	xx	xx	xx	xx	xx	xx	xx	xx	xx	xx	xx
−12	xx	xx	xx	xx	xx	xx	xx	xx	xx	xx	xx	xx	xx	xx	xx	xx	xx	xx	xx	xx	xx	xx	xx	xx
−11	xx	xx	xx	xx	xx	xx	xx	xx	xx	xx	xx	xx	xx	xx	xx	xx	xx	xx	xx	xx	xx	xx	xx	xx
−10	xx	xx	xx	xx	xx	xx	xx	xx	xx	xx	xx	xx	xx	xx	xx	xx	xx	xx	xx	xx	xx	xx	xx	xx
−9	xx	xx	xx	xx	xx	xx	xx	xx	xx	xx	xx	xx	xx	xx	xx	xx	xx	xx	xx	xx	xx	xx	xx	xx
−8	xx	xx	xx	xx	xx	xx	xx	xx	xx	xx	xx	xx	xx	xx	xx	xx	xx	xx	xx	xx	xx	xx	xx	xx
−7	0.05	xx	xx	xx	xx	xx	xx	xx	xx	xx	xx	xx	xx	xx	xx	xx	xx	xx	xx	xx	xx	xx	xx	xx
−6	xx	xx	xx	xx	xx	xx	xx	xx	xx	xx	xx	xx	xx	xx	xx	xx	xx	xx	xx	xx	xx	xx	xx	xx
−5	0.18	xx	xx	xx	xx	xx	xx	xx	xx	xx	xx	xx	xx	0.13	xx	xx	xx	xx	xx	xx	xx	xx	xx	xx
−4	0.45	xx	xx	xx	xx	xx	xx	xx	xx	xx	xx	xx	xx	0.32	xx	xx	xx	0.10	xx	0.07	xx	xx	xx	xx
−3	0.76	xx	xx	xx	xx	xx	xx	0.32	xx	xx	xx	xx	xx	0.48	xx	0.06	xx	0.19	0.08	0.10	0.24	xx	xx	xx
−2	0.62	xx	xx	xx	xx	xx	xx	0.59	xx	xx	xx	xx	xx	0.32	xx	xx	xx	0.15	0.08	0.08	0.43	xx	xx	xx
−1	0.67	xx	xx	xx	xx	xx	xx	0.24	xx	xx	xx	xx	xx	0.33	xx	xx	xx	0.10	0.10	0.07	0.08	xx	xx	0.07
0	0.90	0.06	xx	xx	xx	xx	xx	0.13	xx	xx	xx	xx	xx	0.62	xx	xx	xx	0.18	0.08	0.08	xx	xx	xx	xx
1	0.67	xx	xx	xx	xx	xx	xx	0.21	xx	xx	xx	xx	xx	xx	xx	xx	xx	xx	0.12	0.08	xx	0.08	xx	xx
2	0.62	xx	xx	xx	xx	xx	0.17	0.09	xx	xx	xx	xx	xx	xx	xx	xx	0.07	xx	0.15	xx	xx	xx	xx	xx
3	0.76	0.06	0.05	xx	xx	xx	xx	0.06	xx	xx	xx	xx	xx	xx	xx	xx	xx	xx	xx	xx	0.07	xx	xx	xx
4	0.45	xx	xx	xx	xx	xx	xx	xx	xx	xx	xx	xx	xx	xx	xx	xx	xx	xx	xx	xx	xx	xx	xx	xx
5	0.18	xx	xx	xx	xx	xx	xx	xx	xx	xx	xx	xx	xx	xx	xx	xx	xx	xx	xx	xx	xx	xx	xx	xx
6	xx	xx	xx	xx	xx	xx	xx	xx	xx	xx	xx	xx	xx	xx	xx	xx	xx	xx	xx	xx	xx	xx	xx	xx
7	0.05	xx	xx	xx	xx	xx	xx	xx	xx	xx	xx	xx	xx	xx	xx	xx	xx	xx	xx	xx	xx	xx	xx	xx
8	xx	xx	xx	xx	xx	xx	xx	xx	xx	xx	xx	xx	xx	xx	xx	xx	xx	xx	xx	xx	xx	xx	xx	xx
9	xx	xx	xx	xx	xx	xx	xx	xx	xx	xx	xx	xx	xx	xx	xx	xx	xx	xx	xx	xx	xx	xx	xx	xx
10	xx	xx	0.08	xx	xx	0.07	xx	xx	xx	xx	xx	xx	xx	xx	xx	xx	xx	xx	xx	xx	xx	xx	xx	xx
11	xx	xx	xx	xx	xx	0.13	xx	xx	xx	xx	xx	xx	0.10	xx	xx	xx	xx	xx	xx	xx	xx	xx	xx	xx
12	xx	xx	xx	xx	xx	0.16	xx	xx	xx	xx	xx	xx	xx	0.13	xx	xx	xx	xx	xx	xx	xx	0.20	xx	xx
13	0.70	xx	xx	xx	xx	0.35	xx	xx	xx	xx	xx	0.12	xx	0.22	xx	xx	0.08	xx	xx	xx	0.17	0.29	xx	xx
14	xx	xx	xx	xx	xx	0.31	xx	xx	xx	xx	0.12	xx	xx	0.26	xx	xx	xx	xx	xx	xx	0.10	0.34	xx	xx

Columns record time-lags (correlation with subsequent years, 1 year increment). Rows record space-lags (+ towards Landers, − away from Landers, 10 km increment). Only positive correlation coefficients, statistically significant at the 95% confidence level, are shown.

and had a moment magnitude (M_W) of 7.31. It was centered in the Eastern California Shear Zone, with the hypocenter at 34.2° latitude, −116.43° longitude, and 1.7 km depth. The rupture initiated on the southern Johnson Valley fault, and jumped progressively to the Kickapoo (Landers), Homestead Valley, Emerson and Camp Rock faults. Since we are testing the Stress Accumulation model, we use the same five-segment rupture model that was used by Bowman and King (2001a,b) to document AMR prior to the Landers event (Fig. 1).

We examine the temporal evolution of seismicity rates as a function of distance from the Landers rupture, using the following procedure: The earthquakes are divided into year-long sub-catalogs. The seismicity is then spatially binned according to the distance of the epicenters from the Landers fault trace, in 10 km increments. This separates the sub-catalogs into roughly oblong, concentric rings, centered on the Landers rupture. We then define the short-term, local seismicity rate as the number of events in a given year that fall within the specified ring.

Local seismicity rates on the scale used in our tests are known to vary dramatically. Since it is our interest to evaluate the rate changes over space-time, we do not want sites that are generally more active to wash out any detectable signal from areas having less activity. Furthermore, the association the Stress Accumulation model makes between AMR and the recovery of the area from a stress shadow suggests that the absolute short-term seismicity rate is not as significant as the relationship between that rate and the long-term average. We therefore normalize the rates measured for the spatio–temporal sub-catalogs by the average long-term, regional rate, henceforth called the background rate.

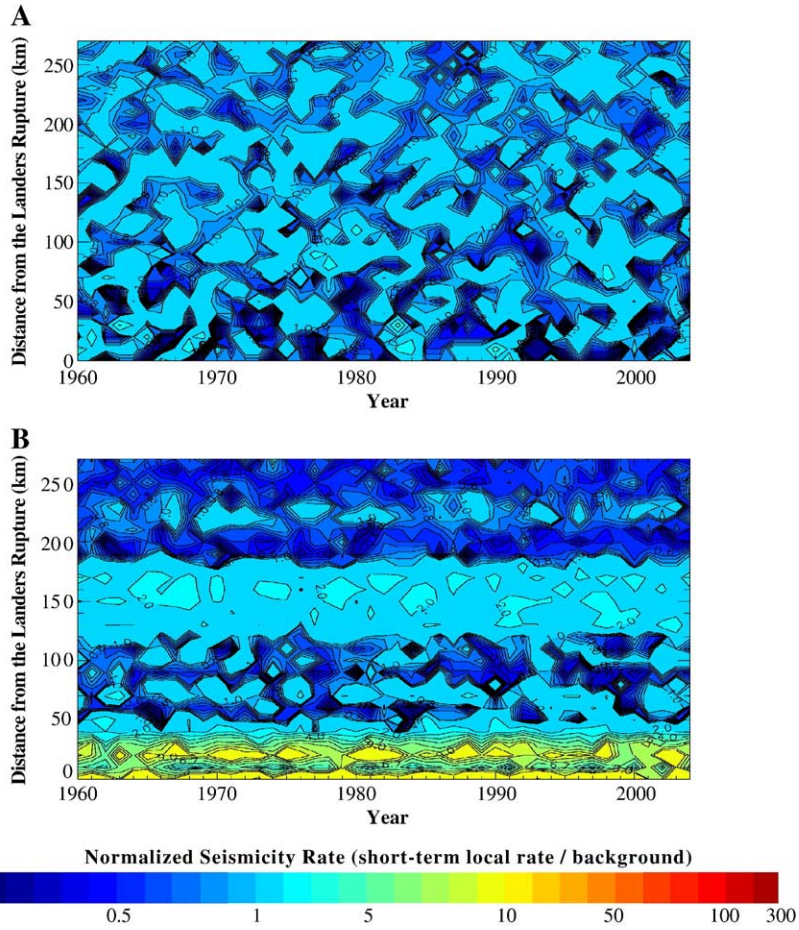

Fig. 3. Yearly seismicity rates for a random catalog, calculated as a function of distance from the Landers rupture and normalized by the long-term, regional background rate. (A) The catalog is generated using a uniform, random distribution to assign times and epicenter locations. (B) Event times are assigned using a uniform, random distribution. Epicenter locations are selected at random from the original catalog, in order to preserve the natural spatial clustering of earthquakes on the fault network.

To estimate the background seismicity rate, we divide the total number of events by the number of years the catalog covers. Comparing the local seismicity rates to this quantity directly would not be meaningful, because the number of earthquakes per year in a small portion of southern California is almost by definition going to be negligible compared to the number of earthquakes per year region-wide. Consequently, we scale the long-term average regional rate by the percentage of the regional area represented by each spatial ring. This percentage increases slightly as the rings sample further distances from the Landers rupture.

A background rate based on the entire seismicity catalog will, of course, include activity from outside the Eastern California Shear Zone, and consequently may not be equivalent to the long-term average in the vicinity of the Landers rupture. It is questionable, though, whether seismicity rates are in fact stable over the long-term at small spatial scales. Since the SA model prediction we are testing explicitly states that the local rates near Landers should *not* be constant over the temporal length of the catalog, the average local seismicity rate is not a physically meaningful quantity. We therefore use the regional rate, which is arguably well represented by the 45 years for which we include data.

In summary, for each spatio–temporal sub-catalog, we calculate the following ratio:

$$\frac{\#\text{ of events in year Y occuring X to X}+10\text{ km from Landers}}{\left(\frac{\text{Total \# of events}}{\text{Total \# of years}}\right)\Big/\left(\frac{\text{Area X to X}+10\text{ km from Landers}}{\text{Total spatial area of the region}}\right)}. \quad (2)$$

The resulting values are stored in a matrix, with rows corresponding to spatial bins and columns to years. To visualize the results, we plot the normalized rates using Research Systems, Inc.'s IDL contouring algorithm.

3. Results

Fig. 2 shows the data for year-long sub-catalogs between 1960 and 2004, compared to a background

Table 2
Coefficients for the lag-shifted auto-correlation of the normalized seismicity rates for a synthetic, random catalog (Fig. 3A)

Lag	0	1	2	3	4	5	6	7	8	9	10	11	12	13	14	15	16	17	18	19	20	21	22	23
−14	xx	xx	xx	xx	xx	0.08	xx	xx	xx	xx	xx	0.09	xx	xx	xx	xx	0.09	xx	xx	xx	xx	xx	xx	xx
−13	xx	xx	xx	xx	xx	xx	xx	xx	xx	xx	xx	xx	0.10	xx	xx	xx	xx	xx	xx	xx	xx	xx	xx	xx
−12	xx	xx	xx	xx	xx	xx	xx	xx	xx	xx	xx	xxx	xx	xx	xx	x	xx	0.09	0.10	xx	xx	xx	xx	xx
−11	xx	xx	0.10	xx	xx	xx	xx	xx	xx	xx	xx	xx	xx	xx	xx	xx	xx	xx	xx	xx	xx	xx	xx	xx
−10	xx	xx	xx	xx	xx	xx	xx	xx	0.09	xx	xx	xx	xx	xx	xx	xx	xx	xx	xx	xx	xx	xx	xx	xx
−9	xx	xx	xx	xx	xx	xx	xx	xx	xx	xx	xx	xx	0.13	xx	xx	xx	xx	xx	xx	xx	xx	xx	xx	xx
−8	xx	xx	xx	xx	xx	xx	xx	xx	xx	xx	xx	xx	xx	xx	xx	xx	xx	xx	xx	xx	xx	0.08	xx	xx
−7	xx	xx	xx	xx	xx	xx	xx	xx	xx	xx	xx	xx	xx	xx	xx	0.07	xx	xx	xx	xx	xx	xx	xx	xx
−6	xx	xx	xx	0.07	xx	xx	xx	xx	xx	xx	xx	xx	xx	xx	0.09	xx	xx	xx	xx	0.11	xx	xx	xx	0.13
−5	xx	xx	xx	xx	xx	xx	xx	0.06	xx	xx	xx	xx	xx	xx	xx	0.08	xx	xx	xx	xx	xx	xx	xx	xx
−4	xx	xx	xx	xx	xx	xx	0.07	xx	xx	xx	xx	xx	xx	xx	xx	xx	xx	xx	xx	xx	xx	xx	xx	xx
−3	xx	xx	xx	0.06	xx	xx	xx	xx	xx	0.06	xx	xx	xx	xx	xx	xx	xx	xx	xx	xx	xx	xx	xx	xx
−2	xx	xx	xx	xx	xx	xx	xx	xx	0.08	xx	xx	xx	xx	xx	xx	0.08	xx	xx	xx	xx	xx	xx	xx	xx
−1	xx	0.09	xx	xx	xx	xx	xx	xx	xx	xx	xx	xx	xx	xx	xx	xx	xx	xx	xx	xx	xx	xx	xx	xx
0	0.90	xx	xx	xx	xx	xx	xx	xx	xx	xx	xx	xx	xx	xx	0.07	xx	xx	xx	xx	xx	0.07	xx	xx	xx
1	xx	xx	xx	xx	xx	xx	xx	xx	xx	xx	xx	xx	xx	xx	xx	xx	xx	xx	xx	xx	xx	xx	xx	xx
2	xx	xx	xx	xx	xx	xx	xx	xx	0.05	xx	xx	xx	xx	xx	xx	0.06	xx	xx	xx	xx	xx	xx	0.07	xx
3	xx	xx	xx	xx	xx	xx	xx	xx	xx	xx	xx	xx	xx	xx	xx	xx	xx	xx	xx	xx	xx	xx	xx	xx
4	xx	0.05	xx	xx	xx	xx	xx	xx	xx	xx	xx	xx	xx	xx	xx	xx	xx	xx	xx	xx	xx	xx	xx	xx
5	xx	xx	xx	xx	xx	xx	xx	xx	xx	xx	xx	xx	xx	xx	0.07	xx	xx	xx	0.07	xx	xx	xx	xx	xx
6	xx	xx	xx	xx	xx	xx	0.07	xx	xx	xx	xx	xx	xx	xx	xx	xx	xx	xx	xx	xx	0.13	0.11	xx	xx
7	xx	xx	xx	xx	xx	xx	xx	xx	xx	xx	xx	xx	xx	xx	xx	xx	xx	xx	xx	xx	xx	xx	xx	xx
8	xx	xx	xx	0.06	0.06	xx	xx	xx	xx	xx	xx	xx	0.09	xx	xx	xx	xx	xx	xx	xx	xx	xx	xx	xx
9	xx	xx	xx	xx	xx	xx	xx	xx	xx	xx	xx	xx	xx	xx	xx	xx	xx	xx	xx	xx	xx	xx	xx	xx
10	xx	xx	xx	xx	0.07	xx	xx	xx	xx	xx	xx	xx	xx	xx	xx	xx	xx	xx	xx	xx	xx	xx	xx	xx
11	xx	xx	xx	xx	xx	xx	xx	xx	xx	xx	xx	xx	xx	xx	xx	xx	xx	xx	xx	xx	0.09	xx	xx	xx
12	xx	0.09	xx	xx	xx	xx	xx	xx	xx	xx	xx	xx	xx	xx	xx	xx	xx	xx	xx	xx	xx	xx	xx	xx
13	xx	xx	xx	xx	xx	xx	xx	xx	xx	xx	xx	xx	xx	xx	xx	xx	xx	xx	xx	xx	xx	xx	xx	xx
14	xx	xx	xx	xx	xx	xx	xx	xx	xx	xx	xx	xx	xx	xx	xx	xx	xx	xx	xx	xx	xx	xx	xx	xx

A uniform random distribution is used to assign the times and epicenter locations of the events. Columns record time-lags (1 year increment).Rows record space-lags (10 km increment). Only positive correlation coefficients, statistically significant at the 95% confidence level, are shown.

rate based on the entire 1960–2004 catalog. Colors towards the red end of the spectrum indicate higher local rates relative to the background. The light blue tone that forms most of the figure's pattern marks the contour for ratios equal to 1.0, or local seismicity rates equivalent to the long-term background rate. The data reveal a number of features of the activity. The aftershock sequences of Landers and the 1999 Hector Mine earthquakes stand out as the highest seismicity rates in the dataset. Within 50 km of the Landers rupture, the seismicity rates are at or above background levels for nearly all space–time bins (with an notable exception in 1982). Between 1960 and 1975, there is a band of activity at/above background levels that appears to migrate from approximately 130 to 70 km from the mainshock. This does follow the SA model prediction, but it is interesting to note that rates drop off at the farther distances as they increase closer in, and they remain fairly stable from 1975 onwards. Perhaps the most striking pattern in the data is the band at 130–170 km, which exhibits semi-periodic pulses of heightened activity. This primarily reflects recurrent seismicity in Imperial Valley and the Transverse Ranges. The highest rates in this band are measured in 1971, 1979, 1987 and 1994. From a surficial view, these correspond to the aftershock sequences of individual, moderate to large magnitude earthquakes. However, it is interesting to note that activity also increased in the Imperial Valley in 1971, when the M_W 6.6, San Fernando earthquake occurred north of the L.A. Basin. Similarly in 1987, the Whittier Narrows event (M_L 5.9) near Los Angeles and the Superstition Hills earthquake (M_W 6.2) in Imperial Valley occurred within two months of each other and virtually equidistant to the future Landers rupture. In contrast, the two regions appear to act independently in 1979 and 1994.

Although the data hints at an inward migration of increased seismicity rates, the pattern of activity is complex and can be interpreted in different ways. To

Table 3
Coefficients for the lag-shifted auto-correlation of the seismicity rates for the earthquake catalog 1960–6/27/92, normalized by the background seismicity rate 1960–2004

Lag	0	1	2	3	4	5	6	7	8	9	10	11	12	13	14	15	16	17
−14	xx	xx	xx	0.13	xx	xx	xx	xx	0.29	xx	xx	xx	xx	xx	xx	xx	0.15	xx
−13	xx	xx	0.08	xx	xx	xx	xx	xx	0.42	xx	xx	xx	0.14	xx	xx	xx	0.12	0.15
−12	xx	xx	xx	xx	xx	xx	xx	xx	0.11	xx	xx	xx	xx	xx	xx	xx	xx	0.15
−11	xx	0.17	xx	xx	xx	xx	xx	xx	xx	xx	xx	xx	xx	xx	xx	xx	xx	xx
−10	xx	xx	xx	xx	xx	xx	xx	xx	xx	xx	xx	xx	xx	xx	xx	xx	xx	xx
−9	xx	xx	xx	xx	xx	xx	xx	xx	xx	xx	xx	xx	xx	xx	xx	xx	xx	xx
−8	xx	xx	xx	xx	xx	xx	xx	xx	xx	xx	xx	xx	xx	xx	xx	xx	xx	xx
−7	xx	xx	xx	xx	xx	xx	xx	xx	xx	xx	xx	xx	xx	xx	xx	xx	xx	xx
−6	xx	xx	xx	xx	xx	xx	xx	xx	xx	xx	xx	xx	xx	xx	xx	xx	xx	xx
−5	xx	xx	xx	xx	xx	xx	xx	xx	xx	xx	xx	xx	xx	xx	xx	xx	xx	xx
−4	xx	xx	xx	xx	xx	xx	xx	xx	xx	xx	xx	xx	xx	xx	xx	xx	xx	xx
−3	xx	xx	xx	xx	xx	xx	xx	0.07	0.1	xx	0.07	0.12	0.08	0.13	0.08	0.23	0.11	0.11
−2	xx	xx	xx	xx	xx	xx	xx	0.18	xx	xx	xx	xx	xx	0.68	xx	xx	xx	0.39
−1	0.41	xx	xx	xx	xx	xx	xx	0.07	xx	xx	xx	xx	xx	0.33	xx	xx	xx	0.21
0	0.9	xx	xx	xx	xx	xx	0.44	xx	0.07	xx	xx	xx	xx	xx	xx	xx	0.09	xx
1	0.41	xx	0.08	xx	xx	0.09	0.31	xx	0.1	xx	xx	xx	xx	xx	0.09	xx	0.12	xx
2	xx	xx	xx	xx	xx	0.08	xx	xx	0.07	xx	xx	xx	xx	xx	xx	xx	0.12	xx
3	xx	xx	xx	xx	xx	xx	xx	xx	xx	xx	xx	xx	xx	xx	xx	xx	xx	xx
4	xx	xx	xx	xx	xx	xx	xx	xx	xx	xx	xx	xx	xx	xx	xx	xx	xx	xx
5	xx	xx	xx	xx	xx	xx	xx	xx	xx	xx	xx	xx	xx	xx	xx	xx	xx	xx
6	xx	xx	xx	xx	xx	xx	xx	xx	xx	xx	xx	xx	xx	xx	xx	xx	xx	xx
7	xx	xx	xx	xx	xx	xx	xx	xx	xx	xx	xx	xx	xx	xx	xx	xx	xx	xx
8	xx	xx	0.1	xx	xx	xx	xx	xx	xx	xx	xx	xx	xx	xx	xx	xx	xx	xx
9	xx	xx	xx	xx	xx	xx	xx	xx	xx	xx	xx	xx	xx	xx	xx	xx	xx	xx
10	xx	xx	xx	xx	xx	xx	xx	xx	xx	xx	xx	xx	xx	xx	xx	xx	xx	xx
11	xx	xx	xx	xx	xx	0.37	xx	xx	xx	xx	xx	0.17	xx	xx	xx	xx	0.12	xx
12	xx	xx	xx	xx	xx	0.29	xx	xx	xx	xx	0.14	0.13	xx	0.12	xx	xx	xx	xx
13	xx	xx	xx	xx	xx	xx	xx	0.11	xx	xx	0.1	xx	xx	0.51	xx	0.22	xx	xx
14	xx	xx	xx	xx	xx	xx	xx	xx	xx	xx	xx	xx	xx	0.44	xx	0.13	xx	xx

Columns record time-lags (1 year increment). Rows record space-lags (10 km increment). Only positive correlation coefficients, statistically significant at the 95% confidence level, are shown.

Table 4
Coefficients for the lag-shifted auto-correlation of the normalized seismicity rates for a random catalog (Fig. 3B)

Lag	0	1	2	3	4	5	6	7	8	9	10	11	12	13	14	15	16	17	18	19	20	21	22	23
−14	0.63	0.62	0.64	0.62	0.64	0.63	0.63	0.65	0.62	0.63	0.63	0.63	0.66	0.63	0.65	0.65	0.63	0.62	0.63	0.65	0.65	0.65	0.65	0.63
−13	0.57	0.57	0.58	0.59	0.59	0.57	0.57	0.57	0.58	0.60	0.58	0.58	0.59	0.61	0.60	0.58	0.59	0.60	0.61	0.60	0.60	0.61	0.60	0.60
−12	0.28	0.27	0.27	0.26	0.26	0.26	0.26	0.26	0.26	0.28	0.27	0.26	0.26	0.24	0.26	0.26	0.26	0.27	0.27	0.26	0.26	0.26	0.25	0.26
−11	0.13	0.11	0.12	0.12	0.12	0.12	0.12	0.13	0.13	0.11	0.13	0.13	0.13	0.12	0.13	0.13	0.14	0.15	0.14	0.13	0.14	0.15	0.15	0.16
−10	xx	xx	xx	xx	xx	xx	xx	xx	xx	xx	xx	xx	xx	xx	xx	xx	xx	xx	xx	xx	xx	xx	xx	xx
−9	xx	xx	xx	xx	xx	xx	xx	xx	xx	xx	xx	xx	xx	xx	xx	xx	xx	xx	xx	xx	xx	xx	xx	xx
−8	xx	xx	xx	xx	xx	xx	xx	xx	xx	xx	xx	xx	xx	xx	xx	xx	xx	xx	xx	xx	xx	xx	xx	xx
−7	xx	xx	xx	xx	xx	xx	xx	xx	xx	xx	xx	xx	xx	xx	xx	xx	xx	xx	xx	xx	xx	xx	xx	xx
−6	xx	xx	xx	xx	xx	xx	xx	xx	xx	xx	xx	xx	xx	xx	xx	xx	xx	xx	xx	xx	xx	xx	xx	xx
−5	xx	xx	xx	xx	xx	xx	xx	xx	xx	xx	xx	xx	xx	xx	xx	0.07	xx	xx	xx	xx	xx	xx	xx	xx
−4	0.18	0.17	0.18	0.20	0.19	0.18	0.20	0.19	0.20	0.20	0.19	0.19	0.20	0.20	0.21	0.19	0.20	0.20	0.20	0.21	0.23	0.21	0.21	0.21
−3	0.63	0.62	0.65	0.64	0.64	0.65	0.64	0.63	0.64	0.63	0.64	0.63	0.63	0.64	0.63	0.65	0.65	0.63	0.62	0.64	0.64	0.61	0.63	0.64
−2	0.71	0.70	0.71	0.71	0.71	0.71	0.71	0.70	0.71	0.71	0.71	0.70	0.70	0.70	0.70	0.69	0.70	0.70	0.70	0.69	0.68	0.69	0.70	0.68
−1	0.60	0.60	0.59	0.60	0.60	0.59	0.59	0.60	0.59	0.60	0.61	0.61	0.59	0.59	0.60	0.62	0.61	0.63	0.63	0.62	0.61	0.61	0.63	0.64
0	0.90	0.92	0.91	0.92	0.93	0.92	0.92	0.93	0.93	0.92	0.92	0.93	0.92	0.91	0.92	0.93	0.93	0.92	0.91	0.90	0.93	0.93	0.91	0.92
1	0.60	0.60	0.59	0.59	0.59	0.60	0.60	0.58	0.58	0.59	0.59	0.60	0.60	0.58	0.60	0.58	0.58	0.59	0.58	0.58	0.59	0.59	0.58	0.57
2	0.71	0.71	0.72	0.71	0.71	0.72	0.70	0.71	0.71	0.71	0.71	0.71	0.71	0.73	0.71	0.72	0.73	0.73	0.73	0.71	0.69	0.70	0.73	0.73
3	0.63	0.64	0.63	0.63	0.63	0.64	0.64	0.63	0.64	0.64	0.62	0.62	0.66	0.63	0.62	0.63	0.63	0.63	0.65	0.64	0.60	0.63	0.66	0.63
4	0.18	0.19	0.19	0.19	0.18	0.18	0.18	0.19	0.19	0.18	0.14	0.16	0.17	0.16	0.16	0.15	0.15	0.14	0.15	0.13	0.14	0.12	0.15	0.16
5	xx	xx	xx	xx	xx	xx	xx	xx	xx	xx	xx	xx	xx	xx	xx	xx	xx	xx	xx	xx	xx	xx	xx	xx
6	xx	xx	xx	xx	xx	xx	xx	xx	xx	xx	xx	xx	xx	xx	xx	xx	xx	xx	xx	xx	xx	xx	xx	xx
7	xx	xx	xx	xx	xx	xx	xx	xx	xx	xx	xx	xx	xx	xx	xx	xx	xx	xx	xx	xx	xx	xx	xx	xx
8	xx	xx	xx	xx	xx	xx	xx	xx	xx	xx	xx	xx	xx	xx	xx	xx	xx	xx	xx	xx	xx	xx	xx	xx
9	xx	xx	xx	xx	xx	xx	xx	xx	xx	xx	xx	xx	xx	xx	xx	xx	xx	xx	xx	xx	xx	xx	xx	xx
10	xx	xx	xx	xx	xx	xx	xx	xx	xx	xx	xx	xx	xx	xx	xx	xx	xx	xx	xx	xx	xx	xx	xx	xx
11	0.13	0.13	0.11	0.11	0.11	0.11	0.10	0.11	0.11	0.11	0.11	0.11	0.10	0.11	0.09	0.08	0.10	0.11	0.09	0.08	0.09	0.12	0.09	0.09
12	0.28	0.28	0.27	0.28	0.28	0.27	0.29	0.28	0.27	0.28	0.29	0.29	0.27	0.28	0.29	0.29	0.28	0.28	0.27	0.29	0.29	0.29	0.28	0.29
13	0.57	0.58	0.58	0.59	0.58	0.58	0.58	0.57	0.58	0.57	0.57	0.58	0.57	0.58	0.56	0.56	0.55	0.55	0.56	0.57	0.55	0.54	0.54	0.55
14	0.63	0.65	0.63	0.62	0.62	0.63	0.62	0.62	0.63	0.62	0.61	0.62	0.61	0.62	0.62	0.61	0.64	0.65	0.62	0.61	0.62	0.61	0.62	0.62

A uniform random distribution is used to assign the event times and epicenters are selected randomly from the real earthquake catalog. Columns record time-lags (1 year increment). Rows record space-lags (10 km increment). Only positive correlation coefficients, statistically significant at the 95% confidence level, are shown.

test the significance of the aforementioned trends, we auto-correlate the data and examine the correlation coefficients for varying spatial and temporal lags. The normalized rates are stored in a matrix, with rows and columns representing the spatial and temporal binning, respectively. We then shift an identical matrix vertically and horizontally across this one by incremental amounts, and cross-correlate the overlapping portions of the two arrays. For a given shift, or lag, of s rows and t columns, the correlation coefficient between the N overlapping array elements is

$$\frac{\sum_{i,j}(x[i,j]-\mu_1)(x[i+s,j+t]-\mu_2)}{N\sqrt{\sigma_1^2\sigma_2^2}} \quad (3)$$

where μ_1 and μ_2 are the mean values for the elements of the original and lag shifted arrays, respectively, that are used in the calculation, and σ_1^2 and σ_2^2 are the associated variances. This equation yields values ranging from -1.0, for perfectly anti-correlated data, to 1.0 for perfect correlation. The closer the value is to zero, the weaker the correlation in the data. In our analyses, the correlation coefficient assesses the persistence of trends in the data across space–time. For example, the correlation coefficient for a lag of $s=2$ and $t=1$ measures the similarity between seismicity rates at one site and the activity occurring one year later and 20 km closer to the Landers rupture. The statistical significance of the correlation is determined using a directional Student's t-distribution test for N element pairs. We focus only on positive correlation coefficients, in order to test the model. The interpretation of anti-correlation in the seismicity rates is beyond the scope of this paper.

Based on the predictions of the SA model, we expect to see a cluster of high, positive correlation values for lags on the order of a few years and small spatial shifts towards Landers. Table 1 shows the positive correlation coefficients that exceed a 95% confidence limit. The high correlation values for 0 time lag and small spatial lags simply indicate that on the scale of one year, seismicity rates tend to be

Table 5
Coefficients for the lag-shifted auto-correlation of the normalized seismicity rates for the earthquake catalog, 1960–2004

Lag	0	1	2	3	4	5	6	7	8	9	10	11	12
−14	xx	0.33	xx	xx	xx	xx	xx	xx	0.12	xx	0.19	xx	xx
−13	xx	0.16	xx	xx	xx	xx	xx	xx	xx	xx	xx	xx	xx
−12	xx	xx	xx	xx	xx	xx	xx	xx	xx	xx	xx	xx	xx
−11	xx	xx	xx	xx	xx	xx	xx	xx	xx	xx	xx	xx	xx
−10	xx	xx	xx	xx	xx	xx	xx	xx	xx	xx	xx	xx	xx
−9	xx	xx	xx	xx	xx	xx	xx	xx	xx	xx	xx	xx	xx
−8	xx	xx	xx	xx	xx	xx	xx	xx	xx	xx	xx	xx	xx
−7	xx	xx	xx	xx	xx	xx	xx	xx	xx	xx	xx	xx	xx
−6	xx	xx	xx	xx	xx	xx	xx	xx	xx	xx	xx	xx	xx
−5	0.19	xx	xx	xx	xx	xx	xx	0.12	xx	xx	xx	xx	xx
−4	0.46	xx	xx	xx	xx	xx	xx	0.33	xx	0.15	xx	xx	xx
−3	0.76	xx	xx	0.31	xx	xx	xx	0.48	xx	0.25	0.3	0.xx	0.16
−2	0.63	xx	xx	0.54	0.08	xx	xx	0.34	xx	0.21	0.46	0.1	0.22
−1	0.67	xx	xx	0.25	xx	xx	xx	0.29	0.08	0.19	0.12	xx	0.17
0	1	xx	xx	0.14	xx	xx	xx	0.48	xx	0.25	0.1	xx	xx
1	0.67	xx	xx	0.18	xx	xx	xx	xx	xx	0.12	0.11	xx	xx
2	63	xx	xx	0.19	xx	xx	xx	xx	xx	0.14	xx	xx	xx
3	0.76	0.07	xx	xx	xx	xx	xx	xx	xx	xx	xx	xx	xx
4	0.46	xx	xx	xx	xx	xx	xx	xx	xx	xx	xx	xx	xx
5	0.19	xx	xx	xx	xx	xx	xx	xx	xx	xx	xx	xx	xx
6	xx	xx	xx	xx	xx	xx	xx	xx	xx	xx	xx	xx	xx
7	xx	xx	xx	xx	xx	xx	xx	xx	xx	xx	xx	xx	xx
8	xx	xx	xx	xx	xx	xx	xx	xx	xx	xx	xx	xx	xx
9	xx	xx	xx	xx	xx	xx	xx	xx	xx	xx	xx	xx	0.13
10	xx	xx	xx	xx	xx	xx	xx	xx	xx	xx	xx	xx	0.15
11	xx	xx	xx	0.12	xx	xx	0.11	xx	xx	xx	xx	xx	0.15
12	xx	xx	0.13	xx	xx	xx	0.12	xx	xx	xx	xx	0.18	0.16
13	xx	xx	xx	xx	xx	xx	xx	xx	xx	xx	xx	xx	xx
14	xx	xx	0.15	0.16	xx	0.16	xx	0.25	xx	xx	xx	0.35	xx

Columns record time-lags (2 year increment). Rows record space-lags (10 km increment). Only positive correlation coefficients, statistically significant at the 95% confidence level, are shown.

Table 6
Coefficients for the lag-shifted auto-correlation of the normalized seismicity rates for the earthquake catalog, 1960–2004

Lag	0	1	2	3	4	5	6	7	8	9	10	11	12	13	14	15	16	17	18	19	20	21	22	23	24	25	26	27	28	29	30	31	32	33	34	35	36	37	38	39	40	41	42	43	44	45
−14	xx	xx	xx	0.13	0.16	xx	0.1	0.13	xx	xx	xx	xx	xx	xx	xx	0.09	xx	xx	xx	xx	xx	xx	xx	xx	xx	xx	xx	xx	xx	xx	xx	0.06	0.12	xx	xx	xx	xx	xx	0.11	xx	0.1	xx	xx	xx	xx
−13	xx	xx	xx	0.1	0.07	xx	xx	0.05	xx	xx	xx	xx	xx	xx	xx	xx	xx	xx	xx	xx	xx	xx	xx	xx	xx	xx	xx	0.06	xx	xx	xx	xx	xx	xx	xx	xx	xx	xx	xx	xx	xx	xx	xx	xx	xx	xx
−12	xx	xx	xx	xx	xx	xx	xx	xx	xx	xx	xx	xx	xx	xx	xx	xx	xx	xx	xx	xx	xx	xx	xx	xx	xx	xx	xx	xx	xx	xx	xx	xx	xx	xx	xx	xx	xx	xx	xx	xx	xx	xx	xx	xx	xx	xx
−11	xx	xx	xx	xx	xx	xx	xx	xx	xx	xx	xx	xx	xx	xx	xx	xx	xx	xx	xx	xx	xx	xx	xx	xx	xx	xx	xx	xx	xx	xx	xx	xx	xx	xx	xx	xx	xx	xx	xx	xx	xx	xx	xx	xx	xx	xx
−10	xx	xx	xx	xx	xx	xx	xx	xx	xx	xx	xx	xx	xx	xx	xx	xx	xx	xx	xx	xx	xx	xx	xx	xx	xx	xx	xx	xx	xx	xx	xx	xx	xx	xx	xx	xx	xx	xx	xx	xx	xx	xx	xx	xx	xx	xx
−9	xx	xx	xx	xx	xx	xx	xx	xx	xx	xx	xx	xx	xx	xx	xx	xx	xx	xx	xx	xx	xx	xx	xx	xx	xx	xx	xx	xx	xx	xx	xx	xx	xx	xx	xx	xx	xx	xx	xx	xx	xx	xx	xx	xx	xx	xx
−8	xx	xx	xx	xx	xx	xx	xx	xx	xx	xx	xx	xx	xx	xx	xx	xx	xx	xx	xx	xx	xx	xx	xx	xx	xx	xx	xx	xx	xx	xx	xx	xx	xx	xx	xx	xx	xx	xx	xx	xx	xx	xx	xx	xx	xx	xx
−7	0.04	xx	xx	xx	xx	xx	xx	xx	xx	xx	xx	xx	xx	xx	xx	xx	xx	xx	xx	xx	xx	xx	xx	xx	xx	xx	xx	xx	xx	xx	xx	xx	xx	xx	xx	xx	xx	xx	xx	xx	xx	xx	xx	xx	xx	xx
−6	xx	xx	xx	xx	xx	xx	xx	xx	xx	xx	xx	xx	xx	xx	xx	xx	xx	xx	xx	xx	xx	xx	xx	xx	xx	xx	xx	xx	xx	xx	xx	xx	xx	xx	xx	xx	xx	xx	xx	xx	xx	xx	xx	xx	xx	xx
−5	0.14	0.09	xx	xx	xx	xx	xx	xx	xx	xx	xx	xx	xx	xx	xx	xx	xx	xx	xx	xx	xx	xx	xx	xx	xx	xx	xx	0.06	xx	xx	xx	xx	xx	xx	xx	xx	xx	xx	xx	xx	xx	xx	xx	xx	xx	xx
−4	0.33	0.23	xx	xx	xx	xx	xx	xx	xx	xx	xx	xx	xx	xx	xx	xx	xx	xx	xx	xx	xx	xx	xx	xx	xx	xx	xx	0.19	xx	xx	xx	xx	xx	xx	0.06	0.07	xx	xx	xx	0.06	xx	xx	xx	xx	xx	xx
−3	0.63	0.42	xx	xx	xx	xx	xx	xx	xx	xx	xx	xx	0.04	0.05	0.28	0.28	0.04	xx	xx	xx	xx	0.06	0.05	xx	xx	xx	0.28	0.33	xx	xx	xx	0.05	xx	xx	0.11	0.13	0.06	0.05	0.05	0.08	0.06	0.28	xx	xx	xx	xx
−2	0.47	0.23	xx	xx	xx	xx	xx	xx	xx	xx	xx	xx	0.04	xx	0.47	0.49	xx	xx	xx	xx	xx	xx	xx	xx	xx	xx	0.24	0.11	xx	xx	xx	xx	xx	xx	0.08	0.08	0.07	xx	0.06	xx	0.1	0.45	xx	xx	xx	xx
−1	0.57	0.26	xx	xx	xx	xx	xx	xx	xx	xx	xx	xx	0.04	0.04	0.17	0.21	xx	xx	xx	xx	xx	xx	xx	xx	xx	xx	0.28	0.11	xx	0.08	xx	xx	xx	0.08	0.05	0.06	0.08	xx	0.05	xx	xx	0.06	xx	xx	xx	xx
0	1	0.42	0.05	0.04	xx	xx	xx	xx	xx	xx	xx	xx	xx	xx	0.1	0.13	xx	xx	xx	xx	xx	xx	xx	xx	xx	xx	0.54	0.3	xx	xx	xx	xx	xx	0.06	0.13	0.12	0.06	0.05	0.06	0.05	xx	xx	xx	xx	xx	xx
1	0.57	0.26	xx	xx	xx	xx	xx	xx	xx	xx	xx	0.05	xx	xx	0.23	0.14	xx	xx	xx	xx	xx	xx	xx	xx	xx	xx	xx	xx	xx	xx	xx	xx	xx	xx	xx	0.05	0.07	0.07	0.05	xx	xx	xx	0.06	0.06	xx	xx
2	0.47	0.28	xx	xx	xx	xx	xx	xx	xx	xx	xx	0.14	0.15	xx	0.09	0.05	xx	xx	xx	xx	xx	xx	xx	xx	xx	xx	xx	xx	xx	xx	xx	xx	xx	0.05	xx	0.1	0.11	xx	xx	xx	xx	xx	xx	xx	xx	xx
3	0.63	0.26	0.05	xx	0.04	0.04	xx	xx	xx	xx	xx	xx	xx	xx	0.06	xx	xx	xx	xx	xx	xx	xx	xx	xx	xx	xx	xx	xx	xx	xx	xx	xx	xx	xx	xx	xx	xx	xx	xx	xx	0.05	xx	xx	xx	xx	xx
4	0.33	0.11	xx	xx	xx	xx	xx	xx	xx	xx	xx	xx	xx	xx	xx	xx	xx	xx	xx	xx	xx	xx	xx	xx	xx	xx	xx	xx	xx	xx	xx	xx	xx	xx	xx	xx	xx	xx	xx	xx	xx	xx	xx	xx	xx	xx
5	0.14	0.04	xx	xx	xx	xx	xx	xx	xx	xx	xx	xx	xx	xx	xx	xx	xx	xx	xx	xx	xx	xx	xx	xx	xx	xx	xx	xx	xx	xx	xx	xx	xx	xx	xx	xx	xx	xx	xx	xx	xx	xx	xx	xx	xx	xx
7	0.04	xx	xx	xx	xx	xx	xx	xx	xx	xx	xx	xx	xx	xx	xx	xx	xx	xx	xx	xx	xx	xx	xx	xx	xx	xx	xx	xx	xx	xx	xx	xx	xx	xx	xx	xx	xx	xx	xx	xx	xx	xx	xx	xx	xx	xx
8	xx	xx	xx	xx	xx	xx	xx	xx	xx	xx	xx	xx	xx	xx	xx	xx	xx	xx	xx	xx	xx	xx	xx	xx	xx	xx	xx	xx	xx	xx	xx	xx	xx	xx	xx	xx	xx	xx	xx	xx	xx	xx	xx	xx	xx	xx
9	xx	xx	xx	xx	xx	xx	xx	xx	xx	xx	xx	xx	xx	xx	xx	xx	xx	xx	xx	xx	xx	xx	xx	xx	xx	xx	xx	xx	xx	xx	xx	xx	xx	xx	xx	xx	xx	xx	xx	xx	xx	xx	xx	xx	xx	xx
10	xx	xx	xx	xx	0.05	0.05	xx	xx	xx	0.06	0.06	xx	xx	xx	xx	xx	xx	xx	xx	xx	xx	xx	xx	xx	0.08	xx	xx	xx	xx	xx	xx	xx	xx	xx	xx	xx	xx	xx	xx	xx	xx	xx	xx	xx	xx	xx
11	xx	xx	xx	xx	xx	xx	xx	xx	xx	0.09	0.06	xx	xx	xx	xx	xx	xx	xx	xx	xx	xx	xx	xx	xx	0.16	xx	xx	xx	xx	xx	xx	xx	xx	xx	xx	xx	xx	0.07	xx	xx	xx	xx	xx	xx	xx	xx
12	xx	xx	xx	xx	xx	xx	xx	xx	0.07	0.13	0.08	xx	xx	xx	xx	xx	xx	xx	xx	xx	xx	xx	xx	xx	0.07	0.07	0.11	xx	xx	xx	xx	xx	xx	xx	xx	xx	xx	xx	xx	xx	0.09	xx	0.1	0.15	xx	xx
13	xx	xx	xx	xx	xx	xx	xx	0.05	xx	0.21	0.21	0.08	xx	xx	xx	xx	xx	xx	xx	xx	xx	xx	0.08	0.1	xx	0.16	0.13	xx	xx	xx	xx	0.1	xx	xx	xx	xx	xx	xx	xx	xx	0.24	xx	0.22	0.14	xx	xx
14	xx	xx	xx	xx	xx	xx	xx	xx	xx	0.1	0.11	0.23	xx	xx	xx	xx	xx	xx	xx	0.07	0.08	xx	xx	xx	xx	0.19	0.16	xx	xx	xx	xx	xx	xx	xx	xx	xx	xx	xx	xx	xx	0.12	xx	0.26	0.2	xx	xx

Columns record time-lags (6 month increment). Rows record space-lags (10 km increment). Only positive correlation coefficients, statistically significant at the 95% confidence level, are shown.

similar across distances on the order of a few tens of kilometers. This is not a surprising result. Otherwise, there is a noticeable lack of correlation for short spatial and temporal lags. Statistically significant correlation is observed for a spatial shift of 30 km towards Landers and temporal lags of 1 and 2 years, but the correlation is very weak.

To further examine the significance of these result, we repeated the analyses using a catalog with the same number of events, randomized in space and time using a uniform random distribution. The bulk of the seismicity rates for the random catalog fall at or below the background rate, and there is no obvious coherent pattern to the fluctuations (Fig. 3A). Nevertheless, the binning procedure and the small size of the region relative to the number of events affect the data such that statistically significant correlation is observed in the rates calculated for the random catalog (Table 2). The correlation values are all very low, and none are clustered in the lag parameter space. However, the coefficients are at least as high as those measured for the real data with lags $[s,t]$ equal to $[3,1]$ and $[3,2]$. In two cases, the random catalog also yields significant correlation for sequential lags, so it appears that level of clustering is not substantial.

We also recalculated the correlation coefficients, including only the data for activity prior to 6/28/92, in order to maximize the sensitivity of the coefficient to the precursory signal (Table 3). With the post-Landers seismicity removed, the correlation for lags $[3,1]$ and $[3,2]$ ceases to be significant. Closer examination of the point by point contribution to the correlation for those lags confirms that the bulk of the correlation comes from the Landers aftershock sequence. In the pre-Landers activity, a weak, but statistically significant correlation is observed for a lag of $[1,2]$, however this is the only significant correlation observed for shifts on the order of a few years and a few tens of kilometers. Thus, we do not find conclusive evidence of the inward migration of seismicity rate increase predicted by the SA model.

Returning to Table 1, it is interesting to note that clusters of significant positive correlation *do* exist in sections of the lag parameter space not explicitly predicted by the SA model. To assess whether or not this clustering could result purely from the spatial association of earthquakes with the existing fault network, we test an additional random catalog, with event times assigned using a random uniform distribution, and epicenters selected at random from the real dataset. The resulting seismicity rates exhibit a strong banding pattern in the spatial domain, but unlike the results for the real data, the rates are fairly uniform in time (Fig. 3B). Although pulses of heightened activity do exist, the distribution of significant correlation coefficients (Table 4) clearly shows that the temporal variability in the random data is inconsequential. (This test was also run using only seismicity prior to 6/28/92 for both the background rate and the randomized epicenters. The absence of the 1992 Landers, 1994 Northridge, and 1999 Hector Mine aftershocks lower the maximum rates observed between 0 and 50 km, but otherwise have no notable impact on the spatial pattern.) We conclude from these tests that the clusters of significant correlation coefficients for the real earthquake catalog are indeed highlighting a statistical feature of the activity related to the underlying earthquake process.

Our choice of a one year time increment and 10 km space increment was a somewhat arbitrary outgrowth of early tests run in the study. To assess the influence of

Table 7
Coefficients for the lag-shifted auto-correlation of the normalized seismicity rates for the earthquake catalog, 1960–2004

Lag	0	1	2	3	4	5	6	7	8	9	10	11	12	13	14	15	16	17	18	19	20	21	22	23
−6	xx	xx	0.56	xx	xx	xx	xx	xx	xx	xx	xx	xx	xx	xx	xx	0.39	xx	xx	xx	0.23	0.36	0.17	xx	xx
−5	xx	xx	0.13	0.11	xx	xx	xx	xx	xx	xx	xx	xx	xx	0.14	xx	xx	xx	xx	xx	xx	xx	xx	xx	xx
−4	xx	xx	xx	xx	xx	xx	xx	xx	xx	xx	xx	xx	xx	xx	xx	xx	xx	xx	xx	xx	xx	xx	xx	xx
−3	xx	xx	xx	xx	xx	xx	xx	xx	xx	xx	xx	xx	xx	xx	xx	xx	xx	xx	xx	xx	xx	xx	xx	xx
−2	xx	xx	xx	xx	xx	xx	xx	xx	xx	xx	xx	xx	xx	0.13	xx	xx	xx	xx	xx	xx	xx	xx	xx	xx
−1	0.87	xx	xx	xx	xx	xx	xx	0.45	xx	xx	xx	xx	xx	0.5	xx	xx	xx	0.17	0.25	0.13	0.25	xx	xx	xx
0	1	xx	xx	xx	xx	xx	xx	0.26	xx	xx	xx	xx	xx	0.5	xx	xx	xx	0.17	0.25	0.13	0.13	xx	xx	xx
1	0.87	xx	xx	xx	xx	xx	0.11	0.21	xx	xx	xx	xx	xx	0.1	xx	xx	xx	xx	xx	xx	xx	xx	xx	xx
2	0.2	xx	xx	xx	xx	xx	xx	xx	xx	xx	xx	xx	xx	xx	xx	xx	xx	xx	xx	xx	xx	xx	xx	xx
3	xx	xx	xx	xx	xx	xx	xx	xx	xx	xx	xx	xx	xx	xx	xx	xx	xx	xx	xx	xx	xx	xx	xx	xx
4	xx	xx	xx	xx	xx	0.1	xx	xx	xx	xx	xx	xx	xx	xx	xx	xx	xx	xx	xx	xx	xx	xx	xx	xx
5	xx	xx	xx	xx	xx	0.45	xx	xx	xx	xx	xx	0.11	xx	0.24	xx	xx	xx	xx	xx	xx	xx	0.35	xx	xx
6	xx	xx	xx	xx	xx	0.16	xx	xx	xx	xx	xx	xx	xx	0.59	xx	xx	xx	xx	xx	xx	0.15	0.68	xx	xx

Columns record time-lags (1 year increment). Rows record space-lags (25 km increment). Only positive correlation coefficients, statistically significant at the 95% confidence level, are shown.

Table 8
Coefficients for the lag-shifted auto-correlation of the normalized seismicity rates for the earthquakes catalog, 1960–2004

Lag	0	1	2	3	4	5	6	7	8	9	10	11	12	13	14	15	16	17	18	19	20	21	22	23	24	25	26	27	28	29	30	31	32	33	34	35	36	37	38	39	40	41	42	43	44	45
−6	xx	0.07	xx	0.36	0.43	xx	xx	xx	xx	xx	xx	xx	xx	xx	xx	xx	xx	xx	xx	xx	xx	xx	xx	xx	xx	xx	xx	xx	xx	0.34	xx	xx	xx	xx	xx	xx	0.11	0.16	0.23	0.14	xx	0.18	xx	xx	xx
−5	xx	xx	xx	0.1	0.07	xx	xx	0.13	xx	xx	xx	xx	xx	xx	xx	xx	xx	xx	xx	xx	xx	xx	xx	xx	xx	xx	0.09	xx	xx	xx	xx	xx	xx	xx	xx	xx	xx	xx	xx	xx	xx	xx	xx	xx	xx	xx
−4	xx	xx	xx	xx	xx	xx	xx	xx	xx	xx	xx	xx	xx	xx	xx	xx	xx	xx	xx	xx	xx	xx	xx	xx	xx	xx	xx	xx	xx	xx	xx	xx	xx	xx	xx	xx	xx	xx	xx	xx	xx	xx	xx	xx	xx	xx
−3	xx	xx	xx	xx	xx	xx	xx	xx	xx	xx	xx	xx	xx	xx	xx	xx	xx	xx	xx	xx	xx	xx	xx	xx	xx	xx	xx	xx	xx	xx	xx	xx	xx	xx	xx	xx	xx	xx	xx	xx	xx	xx	xx	xx	xx	xx
−2	0.14	0.09	xx	xx	xx	xx	xx	xx	xx	xx	xx	xx	xx	xx	xx	xx	xx	xx	xx	xx	xx	xx	xx	xx	xx	xx	0.08	xx	xx	xx	xx	xx	xx	xx	xx	xx	xx	xx	xx	xx	xx	xx	xx	xx	xx
−1	0.78	0.47	xx	xx	xx	xx	xx	xx	xx	xx	xx	xx	0.6	xx	0.34	0.44	xx	xx	xx	xx	xx	xx	xx	xx	xx	xx	0.37	0.26	xx	0.09	xx	xx	xx	xx	0.09	0.19	0.19	xx	0.09	0.09	xx	0.28	xx	xx	xx	xx
0	1	0.45	xx	xx	xx	xx	xx	xx	xx	xx	xx	xx	xx	xx	0.24	0.24	xx	xx	xx	xx	xx	xx	xx	xx	xx	xx	0.44	0.24	xx	0.06	xx	xx	xx	xx	0.11	0.22	xx	0.18	0.07	0.1	xx	xx	0.14	xx	xx	xx
1	0.78	0.26	xx	xx	xx	xx	xx	xx	xx	xx	xx	0.11	0.09	xx	0.22	0.15	xx	xx	xx	xx	xx	xx	xx	xx	xx	xx	0.11	xx	xx	xx	xx	xx	xx	xx	xx	xx	xx	0.04	xx	xx	xx	xx	xx	xx	xx
2	0.14	xx	xx	xx	xx	xx	xx	xx	xx	xx	xx	xx	xx	xx	xx	xx	xx	xx	xx	xx	xx	xx	xx	xx	xx	xx	xx	xx	xx	xx	xx	xx	xx	xx	xx	xx	xx	0	xx	xx	xx	xx	xx	xx	xx	xx
3	xx	xx	xx	xx	xx	xx	xx	xx	xx	xx	xx	xx	xx	xx	xx	xx	xx	xx	xx	xx	xx	xx	xx	xx	xx	xx	xx	xx	xx	xx	xx	xx	xx	xx	xx	xx	xx	0	xx	xx	xx	xx	xx	xx	xx	xx
4	xx	xx	xx	xx	xx	xx	xx	xx	xx	xx	0.09	xx	xx	xx	xx	xx	xx	xx	xx	xx	xx	xx	xx	xx	0.11	xx	xx	xx	xx	xx	xx	xx	xx	xx	xx	xx	0.04	xx	xx	xx	xx	xx	xx	xx	xx	xx
5	xx	xx	xx	xx	xx	xx	xx	xx	xx	0.29	0.23	0.11	xx	xx	xx	xx	xx	xx	xx	xx	xx	xx	xx	0.09	0.09	0.12	0.14	0.18	xx	xx	xx	xx	xx	xx	xx	xx	0.05	xx	xx	0.16	xx	0.22	0.24	xx	xx
6	xx	xx	xx	xx	xx	xx	xx	xx	xx	xx	xx	0.21	xx	xx	xx	xx	xx	xx	xx	xx	xx	xx	xx	xx	xx	0.43	0.41	xx	xx	xx	xx	xx	xx	xx	xx	xx	0	xx	xx	0.18	xx	0.52	0.41	xx	xx

Columns record time-lags (6 month increment). Rows record space-lags (25 km increment). Only positive correlation coefficients statistically at the 95% confidence level, are shown.

those parameter choices on the results, we repeated the analysis using 2 year and 10 km increments (Table 5), 6 month and 10 km increments (Table 6), 1 year and 25 km increments (Table 7), and 6 month and 25 km increments (Table 8). The aforementioned patterns are not as easily distinguishable by visual examination of the data. However, in all four cases, the correlation coefficients show the same banding and semi-periodicity observed in the original test. Furthermore, the additional detail obtained using the smaller time increment suggests that increased activity within 50 km of Landers tends to follow or be followed by pulses of activity around 150 km away with a lag time of about 2 years. This is indicated by (1) high correlation values for spatial shifts outwards of 120–140 km and temporal shifts forwards of 1.5 to 2 years, (2) clusters of high correlation for small spatial shifts and temporal shifts of ~7, ~13.5 and ~18 years (the semi-periodic signal), and (3) clusters of high correlation for spatial shifts inwards of 120–140 km and temporal shifts of ~5, ~12.5 and ~21 years (Table 6).

4. Discussion

The Stress Accumulation model predicts that precursory AMR sequences should have an associated spatio–temporal pattern. Seismicity rates should increase first at the edges of the critical region, gradually increasing at closer distances as time leads up to the next major event. In our analysis of short-term, local seismicity rates prior to the 1992 Landers earthquake, we see some evidence of this trend, for example in the activity from 1960–1975 at 70–130 km distance from the Landers rupture. Lag-shifted auto-correlation does find statistical significance to the trend. However, analysis of random catalog data shows that the observed weak correlation values for isolated space–time lags could simply be a result of the methodology and random fluctuations in the activity.

Although Landers is the largest earthquake in southern California for which we have a substantial dataset of precursory small events, the complexity of its fault history makes it an imperfect test case for the Stress Accumulation model. According to the SA model, the inward migration of seismicity rate increase is specifically a consequence of the erosion of the stress shadow from the last great earthquake. Paleoseismological evidence suggests that the precise rupture that occurred in the Landers earthquake may not have happened in the past. The faults involved, however, do tend to rupture in clusters, with a repeat time on the order of five thousand years (Rockwell et al., 2000). The SA model states

that the stress shadow is primarily eroded through creep on the lower-crustal extension of the main structure but the amount of creep occurring may vary over time. Specifically, creep may advance in the years leading up to a large rupture. Consequently, it is consistent with the model to suggest that a lingering stress shadow existed in the vicinity of Landers. Nevertheless, the fact that the individual faults involved in the Landers earthquake do not consistently rupture in the same combination implies that the stress shadow from prior earthquakes was more spatially heterogeneous than the pattern of stress accumulation predicted by the simply earthquake cycle assumed in the SA model. This may contribute to the weakness of the correlation measured for short space–time lags.

The space- and time-lagged auto-correlation reveals other patterns in the seismicity, though, that require interpretation. Semi-periodicity of peaks in the seismicity rates at 0–50 and 130–170 km shows up in high correlation values for time-lags of 6–7, 13 years, and the larger group of significant correlation coefficients for lags of 17–20 years, which are highest for a lag of 20 years. The spread of the correlation values in the spatial domain likely reflects the width of these "active" bands, which the results shown in Fig. 3B suggest are related to a spatial scale inherent to the southern California fault network.

Perhaps the most intriguing result of the correlation analysis is the 1.5–2 year offset of clusters of high correlation within the spatial bands with clusters of high correlation between the spatial bands. A cursory examination of the data suggests that the source of the correlation is primarily from activity in Imperial Valley, the Transverse Ranges and the Eastern California Shear Zone. Although correlation does not necessarily equal causation, the implication that seismicity in the Eastern California Shear Zone effects and is effected by increased activity in Imperial Valley and Transverse Ranges warrants further investigation.

5. Conclusions

The Stress Accumulation model presents a physical explanation for the observation of accelerating moment release prior to large earthquakes. The model associates AMR with the evolution of the stress field around the mainshock fault in response to aseismic slip on the lower-crustal extension of the fault. This slip in the lower crust simultaneously loads the locked upper portion of the fault, and erodes the stress shadow in the surrounding crust from the previous large earthquake. The SA model states further that the erosion of the stress shadow should cause seismicity rates to increase at progressively closer distances to the main fault as time approaches the next major event. We test this prediction of the SA model by examining yearly seismicity rates as a function of distance from the Landers rupture. To assess the significance of trends in the results, we auto-correlate the data, incorporating spatial and temporal lags. We do measure weak, but statistically significant correlation for rates separated by a few years and a few tens of kilometers in the direction of Landers. However, we can obtain a similar level of correlation by applying our methodology to a random catalog, suggesting that slight correlation may be caused by the binning procedure. Thus, our results do not conclusively support the SA model.

Unexpected results of the analysis include the observation of significant semi-periodicity in the rate fluctuations, as well as strong correlation between seismicity rates 130–170 km from Landers and activity within 50 km of Landers, with a temporal lag of 1.5–2 years. Whether or not these spatio–temporal length scales reflect the physics of a "communication" process within the fault network will be the subject of future research.

Acknowledgments

We would like to thank Greg Anderson, Charles Bufe, and an anonymous reviewer for providing insightful recommendations. We would also like to acknowledge many hours of useful discussion with Kristy Tiampo. This work was supported by NSF Grants EAR-9902901 (C.G.S.) and EAR 0107129 (D.D.B.), and by the Southern California Earthquake Center through cooperative agreement EAR-01016924 and the United States Geological Survey cooperative agreement 02HQA60008. The SCEC contribution number for this paper is 937.

References

Anghel, M., Klein, W., Rundle, J.B., Sá Martins, J.S., 2000. Scaling in a Cellular Automaton Model of Earthquake Faults, Cond-Mat/0002459, vol. 1.

Ben-Zion, Y., Lyakhovsky, V., 2002. Accelerated seismic release and related aspects of seismicity patterns on earthquake faults. Pure Appl. Geophys. 159, 2385–2412.

Bowman, D.D., King, G.C.P., 2001a. Accelerating seismicity and stress accumulation before large earthquakes. Geophys. Res. Lett. 28 (21), 4039–4042.

Bowman, D.D., King, G.C.P., 2001b. Stress transfer and seismicity changes before large earthquakes. C. R. Acad. Sci. Paris 333, 591–599.

Bowman, D.D., Sammis, C.G., 2004. Intermittent criticality and the Gutenberg–Richter distribution. Pure Appl. Geophys. 161, 1945–1956. doi:10.1007/s00024-004-2541-z.

Bowman, D.D., Ouilon, G., Sammis, C.G., Sornette, A., Sornette, D., 1998. An observational test of the critical earthquake concept. J. Geophys. Res. 103, 24,359–24,372.

Bowman, D.D., Clark, J., Ikeda, N., 2003. Accelerating moment release as a tool for seismic hazard assessment in southern California. Paper presented at the 2003 Annual Meeting, Southern California Earthquake Center, Oxnard, Calif. (7–11 Sept.).

Bufe, C.G., Varnes, D.J., 1993. Predictive modeling of the seismic cycle for the greater San Francisco Bay region. J. Geophys. Res. 98, 9871–9883.

Bufe, C.G., Nishenko, S.P., Varnes, D.J., 1994. Seismicity trends and potential for large earthquakes in the Alaska–Aleutian region. Pure Appl. Geophys. 142, 83–99.

Clark, J., Bowman, D., King, G., Sammis, C., 2003. Accelerating moment release as a tool for seismic hazard assessment in southern California. Geophys. Res. Abs. 5, 7422.

Dieterich, J., 1994. A constitutive law for rate of earthquake production and its application to earthquake clustering. J. Geophys. Res. 99 (B2), 2601–2618.

Ellsworth, W.L., Lindh, A.G., Prescott, W.H., Herd, D.J., 1981. The 1906 San Francisco earthquake and the seismic cycle. In: Simpson, D.W., Richards, P.G. (Eds.), Earthquake Prediction: an International Review, Maurice Ewing Ser., vol. 4, pp. 126–140.

Helmstetter, A., 2003. Is earthquake triggering driven by small earthquakes? Phys. Rev. Lett. 91 (5), 058501.

Helmstetter, A., Sornette, D., 2002. Sub-critical and super-critical regimes in epidemic models of earthquake aftershocks. J. Geophys. Res. 107 (B10), 2237. doi:10.1029/2001JB001580.

Helmstetter, A., Sornette, D., 2003. Importance of direct and indirect triggered seismicity. Geophys. Res. Lett. 30 (11), 1576. doi:10.1029/2003GL017670.

Huang, Y., Saleur, H., Sammis, C.G., Sornette, D., 1998. Precursors, aftershocks, criticality and self-organized criticality. Europhys. Lett. 41, 43–48.

Kagan, Y.Y., Knopoff, L., 1987. Statistical short-term earthquake prediction. Science 236, 1563–1567.

King, G.C.P., Bowman, D.D., 2003. The evolution of regional seismicity between large earthquakes. J. Geophys. Res. 108 (B2). doi:10.1029/2001JB000783.

Knopoff, L., Levshina, T., Keilis-Borok, V.I., Mattoni, C., 1996. Increased long-range intermediate-magnitude earthquake activity prior to strong earthquakes in California. J. Geophys. Res. 101, 5779–5796.

Lindh, A.G., 1990. The seismic cycle pursued. Nature 348, 580–581.

Lyakhovsky, V., Ben-Zion, Y., Agnon, A., 1997. Distributed damage, faulting and friction. J. Geophys. Res. 102, 27,635–27,649.

Ogata, Y., 1988. Statistical models for earthquake occurrence and residual analysis for point processes. J. Am. Stat. Assoc. 83, 9–27.

Ogata, Y., Matsu'ura, R.S., Katsura, K., 1993. Fast likelihood computation of epidemic type aftershock sequence model. Geophys. Res. Lett. 20 (19), 2143–2146.

Reid, H.F., 1910, The mechanics of the earthquake: the California earthquake of April, 18, 1906, Report of the State Investigation Commission, v.2, Carnegie Institution of Washington.

Robinson, R., 2000. A test of the precursory accelerating moment release model on some recent New Zealand earthquakes. Geophys. J. Int. 140, 568–576.

Rockwell, T.K., Lindvall, S., Herzberg, M., Murbach, D., Dawson, T., Berger, G., 2000. Paleoseismology of the Johnson Valley, Kickapoo, and Homestead Valley faults: Clustering of earthquakes in the Eastern California Shear Zone. Bull. Seismol. Soc. Am. 90 (5), 1200–1236.

Rundle, J.B., Tiampo, K.F., Klein, W., Sa Martins, J.S., 2002. Self-organization in leaky threshold systems: the influence of near-mean field dynamics and its implications for earthquakes, neurobiology, and forecasting. Proc. Natl. Acad. Sci. 99, 2514–2521.

Sammis, C.G., Smith, S.W., 1999. Seismic cycles and the evolution of stress correlation in cellular automaton models of finite fault networks. Pure Appl. Geophys. 155, 307–334.

Sammis, C.G., Sornette, D., Saleur, H., 1996. Complexity and earthquake forecasting. In: Rundle, J., Turcotte, D., Klein, W. (Eds.), Reduction and Predictability of Natural Disasters. Addison–Wesley, pp. 143–156.

Sammis, C.G., Bowman, D.D., King, G.C.P., 2004. Anomalous seismicity and accelerating moment release preceding the 2001 and 2002 earthquakes in Northern Baja California, Mexico, Pure Appl. Geophys. 161, 2369–2378.

Sornette, D., Sammis, C.G., 1995. Complex critical exponent from renormalization group theory of earthquakes: implications for earthquake predictions. J. Phys. I. France 5, 607–619.

Sykes, L.R., Jaumé, S.C., 1990. Seismic activity on neighbouring faults as a long-term precursor to large earthquakes in the San Francisco Bay area. Nature 348, 595–599.